1. Specification of figures in folders

The Supplement includes all figures that are not shown in the paper. Figures present the performance of the representations of the three subsurface processes discussed in the paper under different climate conditions and soil properties of three sites, different scales, and different hillslope configurations. Figures compare modeled hydrological quantities in time series and correlation.

- The three subsurface processes discussed in this paper are:
  (1) assuming ice has equal density with liquid water
  (2) neglecting cryosuction effect in unsaturated soil during soil freezing
  (3) neglecting advective heat transport
- The three sites are:
  (1) Utqiagvik (Barrow Environmental Observatory)
  (2) the headwaters of the Sagavanirktok (Sag) River
  (3) the Teller Road Mile Marker 27 site on the Seward Peninsula of Alaska
- Model were setup based on two scales:
  (1) Column scale representing expansive flat regions
  (2) Hillslope scale representing hilly terrain
- Hillslope scenarios include four configurations:
  (1) Northern aspect, convergent hillslope
  (2) Northern aspect, divergent hillslope
  (3) Southern aspect, convergent hillslope
  (4) Southern aspect, divergent hillslope
- Quantities compared in figures:
  (1) Evaporation rate (mm/d)
  (2) Hillslope downstream outlet discharge (m^3/d)
  (3) Thaw depth (cm)
  (4) Total water saturation, including ice and liquid, at 5 cm beneath soil surface (m^3/m^3)
  (5) Surface temperature (K)
  (6) Soil temperature at 1 m beneath soil surface (K)

2. Grid convergence

Grid convergence study was conducted, and the discretization error was compared with the “error”

caused by omitting a given process. This comparison was done for the column mesh and the southern-aspect divergent hillslope mesh under the Sag River conditions. Thaw depth, as a significant permafrost concept, was used as the evaluation quantity for the comparison.

For the column model (50 m deep), we generated five meshes. From the coarsest to the finest, the numbers of cells are 20, 39, 78, 156, 312. We used 78 cells in the paper. Column models with these different numbers of cells were conducted with full physics representations. For the 78-cells column model, we also conducted simulations with simplified representation for each physical process, i.e., equal liquid-ice density, neglecting advective heat transport, and neglecting cryosuction effect, which has been discussed in the paper. The column model with the finest mesh was assumed to output the most accurate results. All other column models with full physics representations were compared to the finest model. The 10-year averaged absolute error in thaw depth was calculated and shown in Figure S2.1. Figure S2.1 illustrates the relation between error and numbers of cells in double logarithmic coordinates. Black points are discretization errors relative to the finest column model, which are almost on the same line, demonstrating the expected first order convergence rate (due to first-order upwinding methods being used in both the advective term and the relative permeability). The blue, red, and green points show the errors caused by each physics simplification, respectively. Clearly the error due to process omission is comparable to the discretization error in the first two cases, but not in the cryosuction case. This supports the conclusion that cryosuction is crucial. It also demonstrates that our measured differences in advective heat transport and equal liquid and ice densities are, at best, upper bounds on the true differences – they may in fact be smaller.

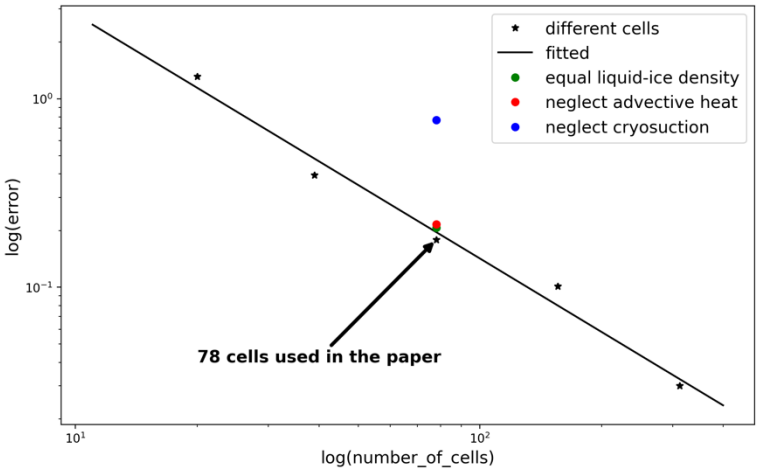

S2.1 Average error in thaw depth caused by numbers of cells and physical process representations for column models under site Sag's condition

Additionally, we also performed the same grid convergence study for a hillslope model. The south facing divergent hillslope mesh was selected to maximize the dynamic range of the system. We generated five meshes with different numbers of cells, from the coarsest to the finest, which are 1050, 1950, 3900, 7800, 15600, and we used 3900 cells for hillslope meshes in the paper. The five hillslope models were conducted with full physics representations, and we also have the 3900-cell hillslope model with simplified physics representations as discussed in the paper. The results obtained using the finest mesh was considered the most accurate and the other four models with coarser meshes were compared with it. The black points in Figure S2.2 are the 10-year averaged absolute errors in thaw depth for the four hillslope models with different numbers of meshes. They are almost on the same line demonstrating the spatial resolution has little impact on solutions. Similar results to the column model are shown, though the error associated with neglecting advective heat transport and liquid-ice density have grown slightly relative to the discretization error, hinting (but not conclusively proving) that these may be closer to true measures of the error than upper bounds on the error.

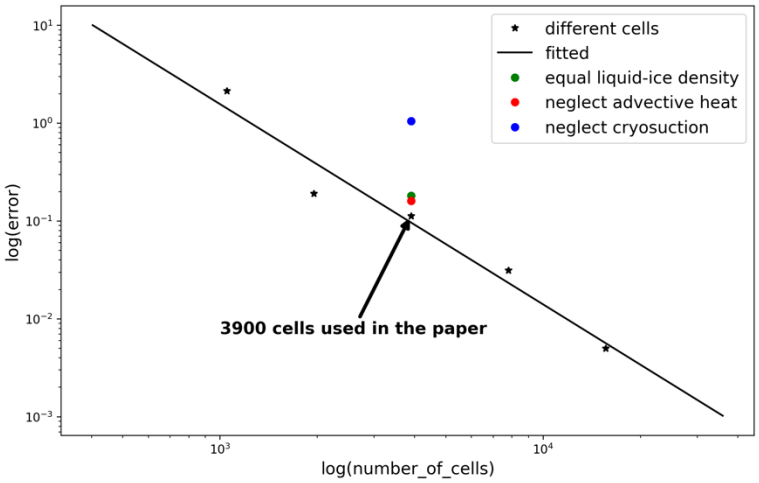

S2.2 Average error in thaw depth caused by number of cells and physical process representations for southern-aspect divergent hillslope models under site Sag's condition.

3. Supplement figures for Section 4.2 of the manuscript

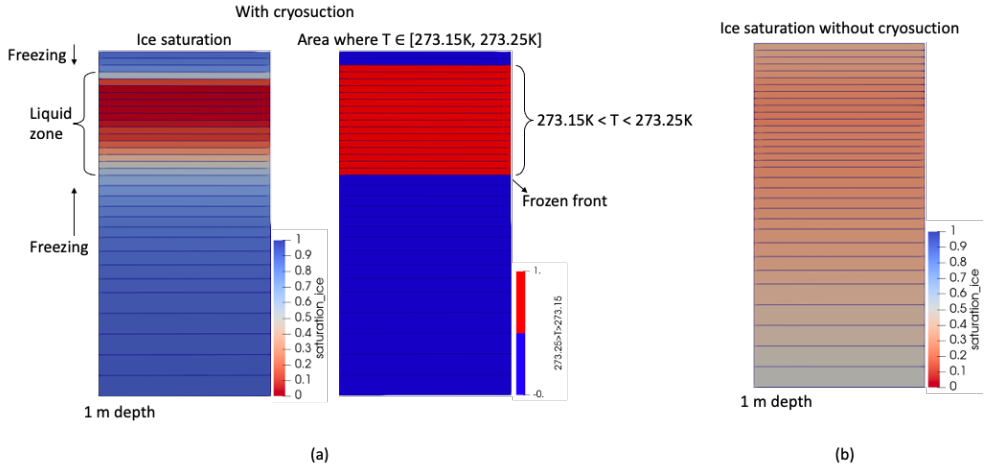

Figure S3.1 (a) Ice saturation and area where temperature is between 273.15K and 273.25K within the top 1 m depth of a column model under Sag's condition at DOY = 300, with cryosuction process in simulation (DOY is day of year); (b) Ice saturation within the top 1 m depth of a column model under Sag's condition at DOY = 300, without cryosuction process in simulation.

4. Supplement figures for Section 4.3 of the manuscript

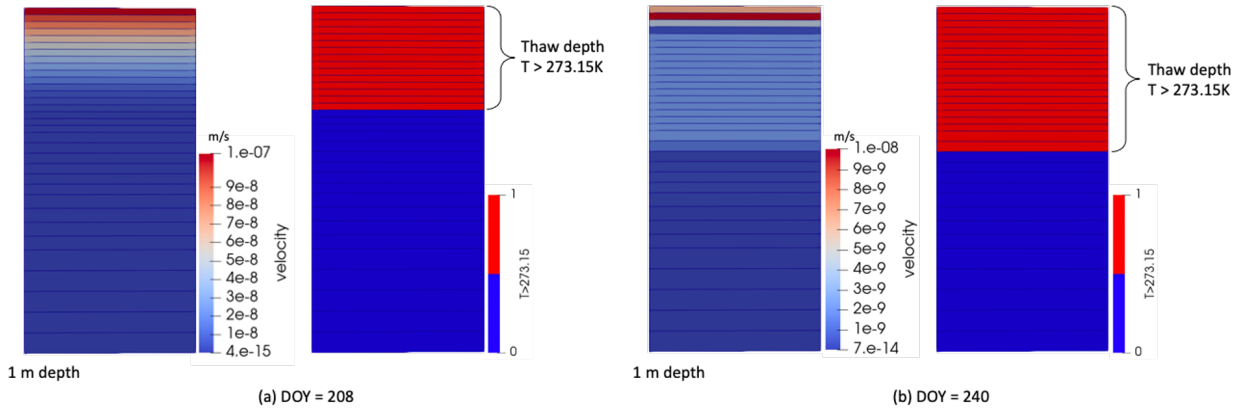

Figure S4.1 Vertical velocity distribution and thaw depth within the top 1m depth of a column model under Sag's condition at DOY = 208 and 240.

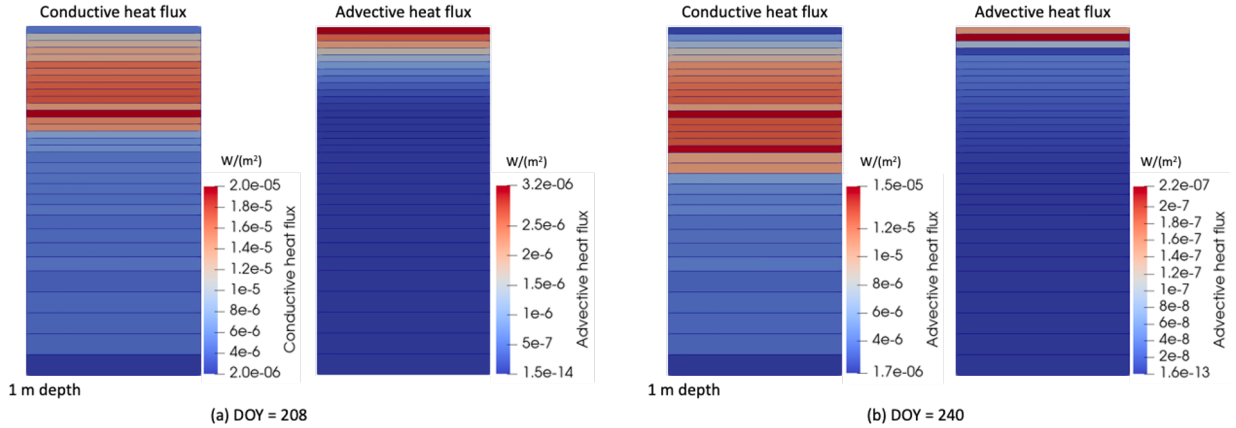

Figure S4.2 Absolute value of conductive and advective heat flux within the top 1m depth of a column model under Sag's condition at DOY = 208 and 240.